Inorganic Chemistry

pubs.acs.org/IC Article

# Microwave Synthesis and Magnetocaloric Effect in $AlFe_2B_2$

Dallas K. Mann, YiXu Wang, Jeanette D. Marks, Geoffrey F. Strouse, and Michael Shatruk*

Cite This: *Inorg. Chem.* 2020, 59, 12625−12631 Read Online

ACCESS | Metrics & More | Article Recommendations | Supporting Information

**ABSTRACT:** A promising magnetic refrigerant, $AlFe_2B_2$, has been prepared for the first time by microwave (MW) melting of a mixture of constituent elements. For comparison, samples of $AlFe_2B_2$ have been also prepared by arc-melting, traditionally used for the synthesis of this material, and by induction (RF) melting, which was used in the very first report on the synthesis of $AlFe_2B_2$. Although an excess of Al has to be used to suppress the formation of ferromagnetic FeB, the other byproduct, $Al_{13}Fe_4$, is easily removed by acid treatment, affording phase-pure samples of $AlFe_2B_2$. Our analysis indicates that the equimolar Fe/B ratio typically used for the preparation of $AlFe_2B_2$ might not provide the best synthetic conditions, as it does not account for the full reaction stoichiometry. Furthermore, we find that the initial Al/Fe loading ratio strongly influences magnetic properties of the sample, as judged by the range of ferromagnetic ordering temperatures ($T_C$ = 280−293 K) observed in our experiments. The $T_C$ value increases with the decrease in the Al/Fe ratio, due to the change in the Al/Fe antisite disorder. The use of the same Al/Fe loading ratio in the arc-, RF-, and MW-melting experiments leads to samples with a more consistent $T_C$ of 286−287 K and similar values of the magnetocaloric effect.

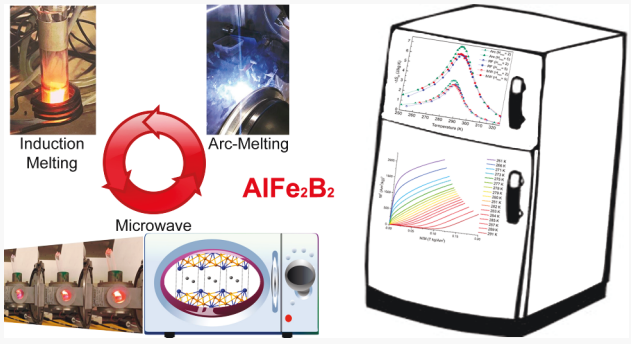


## INTRODUCTION

Room-temperature magnetic refrigeration is an appealing emerging technology that improves on current vapor compression refrigerants by offering higher cooling efficiencies and eliminating the emission of greenhouse gases.[1] This cooling method relies on the magnetocaloric effect (MCE), first reported by Weiss and Piccard in 1917.[2] The MCE is characterized as a reversible adiabatic temperature change or a reversible isothermal entropy change upon application and removal of an external magnetic field. The research on magnetocalorics has skyrocketed since 1997, with the discovery of a giant MCE near room temperature (RT) in $Gd_5Si_2Ge_2$.[3] Since then, a number of other giant-MCE materials have come to the forefront of this research area, although many of them contain expensive or toxic elements.[4−6]

In recent years, $AlFe_2B_2$ has become one of the most investigated systems among magnetocalorics composed of earth-abundant elements.[7,8] The near-RT magnetic ordering and soft ferromagnetism observed for this material are desirable parameters for the practical implementation of magnetocalorics in household cooling technologies. Nevertheless, despite the progress made in understanding the magnetic structure[9] and the nature of magneto-structural coupling[10] associated with the FM ordering in $AlFe_2B_2$, the synthesis of this material remains thwarted by the presence of impurity phases, such as FeB and $Al_{13}Fe_4$, which exhibit ferromagnetism and paramagnetism, respectively, at the Curie temperature ($T_C$) of $AlFe_2B_2$.[11]

The presence of FeB in the arc-melted samples of $AlFe_2B_2$ can be avoided by using an excess of aluminum, while the $Al_{13}Fe_4$ byproduct can be dissolved in dilute hydrochloric acid (HCl). Using this approach, our group achieved the first synthesis of phase-pure bulk $AlFe_2B_2$.[7] In the same work, we also demonstrated that phase-pure $AlFe_2B_2$ could be obtained by a stoichiometric reaction between elements in Ga flux, which was subsequently removed by treatment with a solution of iodine in *N*,*N*-dimethyformamide (DMF). In contrast to arc-melting, this method is more laborious, albeit Ga, if desired, can be almost quantitatively recovered by chemical or electrochemical reduction of the obtained $GaI_3$ solution in DMF.

Given the growing interest to the magnetocaloric properties of $AlFe_2B_2$, we have considered alternative protocols for the synthesis of this material, which, thus far, has been commonly obtained by arc-melting.[12] Only a few works reported alternative methods. Beyond the aforementioned synthesis in Ga flux, $AlFe_2B_2$ was also prepared in Al flux (in a so-called self-flux process), which allowed the growth of sufficiently large single crystals.[13−15] Application of spark-plasma sintering

Received: June 11, 2020
Published: August 13, 2020

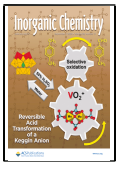







https://dx.doi.org/10.1021/acs.inorgchem.0c01731
*Inorg. Chem.* 2020, 59, 12625−12631

allowed the synthesis of compacted powder and partial substitution of Co for Fe, which was challenging to achieve by arc-melting.[15] Melt-spinning of a stoichiometric mixture was claimed to lead to a nearly phase-pure $AlFe_2B_2$, with less than 2% of FeB impurity.[16] Surprisingly, no efforts have been reported to reproduce the very first synthesis of $AlFe_2B_2$ by Jeitschko, who obtained single crystals of this material by induction (RF) melting.[17] Driven by this lapse, we set out to reinvestigate the synthesis of $AlFe_2B_2$ by RF-melting, as well as to apply a more accessible technique appropriate for fast heating of metal-containing compositions, i.e., microwave (MW) melting. Applications of MW heating to the synthesis of solid-state materials are likely to expand, given the simplicity of the experimental setup and rapid and uniform heating of samples afforded by MW irradiation.[18] Herein, we describe a comparative study of the synthesis and magnetic properties of $AlFe_2B_2$ obtained by arc-, RF-, and MW-melting. We demonstrate that the MW technique allows for the rapid synthesis of $AlFe_2B_2$, with the quality of the material comparable to that obtained by the more traditional arc-melting method.

## MATERIALS AND METHODS

**Starting Materials.** All manipulations during sample preparation were carried out in an Ar-filled drybox (content of $O_2$ < 0.5 ppm). Powders of aluminum (99.97%), iron (99.8%), and crystalline boron (98%) were obtained from Alfa Aesar. The iron powder was additionally purified by heating in a flow of $H_2$ gas at 500 °C for 5 h. The other materials were used as received.

**Method 1: Arc-Melting.** Starting materials were mixed in Al/Fe/B ratios of 3:2:2 and 3:2.6:2 (the total mass of each sample was 0.35 g) and pressed into pellets. Each pellet was arc-melted under argon and flipped each time between 4 consecutive meltings to ensure uniform processing. The resulting ingots were sealed under vacuum (~$10^{-4}$ Torr) in fused silica tubes of 10 mm inner diameter (i.d.) and subjected to homogenizing annealing at 900 °C for 1 week, followed by cooling to RT in a switched-off furnace.

**Method 2: Induction (RF) Melting.** Starting materials were mixed in Al/Fe/B ratios of 7:7:6 and 3:2.6:2 (the total mass of each sample was 0.35 g) and pressed into pellets. Each pellet was loaded into an alumina crucible (3 mL) that was placed into a larger alumina crucible with Ta foil lining the space between the walls of two crucibles. The assembly was suspended inside a silica tube placed in the center of a 3 kW radio frequency (RF) coil (Hüttinger) inside an Ar-filled drybox. The temperature of the sample was monitored with a pyrometer. The pellet was heated to ~1600 °C in ~12 min, kept at that temperature for 1 h, and cooled to RT at ~50 °C/min. Homogenizing annealing of the ingot was performed as described in Method 1: Arc-Melting.

**Method 3: Microwave (MW) Melting.** Starting materials were mixed in the Al/Fe/B ratio of 3:2.6:2 (the total mass of the sample was 0.50 g), pressed into a pellet, and loaded into an alumina crucible (3 mL). The crucible was sealed under vacuum (~$10^{-4}$ Torr) in a fused silica tube of 10 mm i.d. Dry glass wool was loaded below and above the alumina crucible to prevent possible collapse of the silica tube during rapid MW heating of the sample. The tube was placed in a MW reactor operating at 0.5 kW and heated for 5 min, after which the reactor was turned off. After cooling to RT, the tube was open in air, and the sample was transferred to a new silica tube, sealed under vacuum, and subjected to homogenizing annealing as described in Method 1: Arc-Melting.

The samples obtained by all three methods contained $Al_{13}Fe_4$ byproduct, which was removed by stirring each sample in a dilute HCl solution (1:1 v/v) for ~10 min, following the protocol described earlier.[7] The phase purity of the resulting samples was confirmed by powder X-ray diffraction (PXRD).

**Powder X-ray Diffraction.** Room-temperature PXRD was carried out on a Panalytical X'Pert Pro diffractometer with an X'Celerator detector using Cu K$\alpha$ radiation ($\lambda$ = 1.54187 Å). Each pattern was recorded in the 2$\theta$ range from 10° to 80° with a step of 0.05° and the total collection time of 1 h. The analysis of PXRD patterns was carried out with the HighScore Plus software (Panalytical).[19]

**Physical Measurement.** Elemental analysis was carried out on a JEOL 5900 scanning electron microscope with an energy-dispersive X-ray (EDX) microanalysis. All magnetic measurements were performed on polycrystalline samples using a Quantum Design SQUID magnetometer MPMS-XL. Temperature-dependent magnetization was measured in the range of 1.8−390 K under an applied field of 0.01 T. To calculate the MCE values, magnetization isotherms were recorded at temperatures 40 K above and below the Curie temperature ($T_C$) of each sample, with the magnetic field varied from 0 to 5 T. The temperature was changed in a variable increment, with smaller steps taken around the $T_C$.

## RESULTS AND DISCUSSION

**Synthesis of $AlFe_2B_2$.** The most conventional method used for the synthesis of $AlFe_2B_2$ is arc-melting (see Table 1 and references therein). Under stochiometric conditions, the major phase formed is $AlFe_2B_2$, but one also observes $Al_{13}Fe_4$ or FeB as byproducts, depending on the Al/Fe/B ratio. The presence of FeB is problematic, as it is extremely difficult to eliminate this compound from the product mixture. Therefore, an excess of Al has been used to suppress the formation of FeB.[7,8] For example, annealing a sample with the Al/Fe/B ratio of 3:2:2 results in the formation of $AlFe_2B_2$ contaminated only with $Al_{13}Fe_4$. The latter can be readily removed by treating the mixture with dilute HCl (1:1 v/v). The treatment should be kept short (~10 min) to avoid the loss of $AlFe_2B_2$, which also dissolves in dilute HCl but at a much slower rate. A comparison of PXRD patterns at different stages of the

**Table 1. Summary of Works That Reported the Synthesis of Phase-Pure $AlFe_2B_2$**

| synthesis method | post-annealing (yes/no) | Al/Fe/B ratio | acid treated (yes/no) | reference |
|---|---|---|---|---|
| arc-melting | Y | 3/2/2 or 3/2.6/2 | Y | this work |
| RF-melting | Y | 7/7/6 or 3/2.6/2 | Y | |
| MW-melting | Y | 3/2.6/2 | Y | |
| arc-melting | Y | 3/2/2 | Y | 7 and 21 |
| annealing (Ga flux) | Y | 1.5/1.8/2 (+10 Ga) | Y | 7 |
| arc-melting | Y | 1.5/2 (Al/FeB) | Y | 9 |
| arc-melting | Y | 3/2/2 | Y | 22 |
| annealing (self-flux) | Y | 5/3/2 | Y | 13 |
| annealing (self-flux) | Y | 1.5/1.5/2 | Y | 14 |
| arc-melting | Y | 1.5/2/2 | Y | 23 |
| arc-melting | Y | (2−3)/2/2 | Y | 15 |
| annealing (self-flux) | Y | (2−6)/2/2 | Y | |
| melt-spinning | Y | 1/2/2 | N | 16 |
| arc-melting | Y | 1.5/2 (Al/FeB) | Y | 24 |
| arc-melting | Y | 1.2/2/2 | N | 11 |
| RF-melting[a] | N | 7/7/6 | Y | 17 |

[a]Crystals were selected from a multiphase sample.


https://dx.doi.org/10.1021/acs.inorgchem.0c01731
Inorg. Chem. 2020, 59, 12625−12631

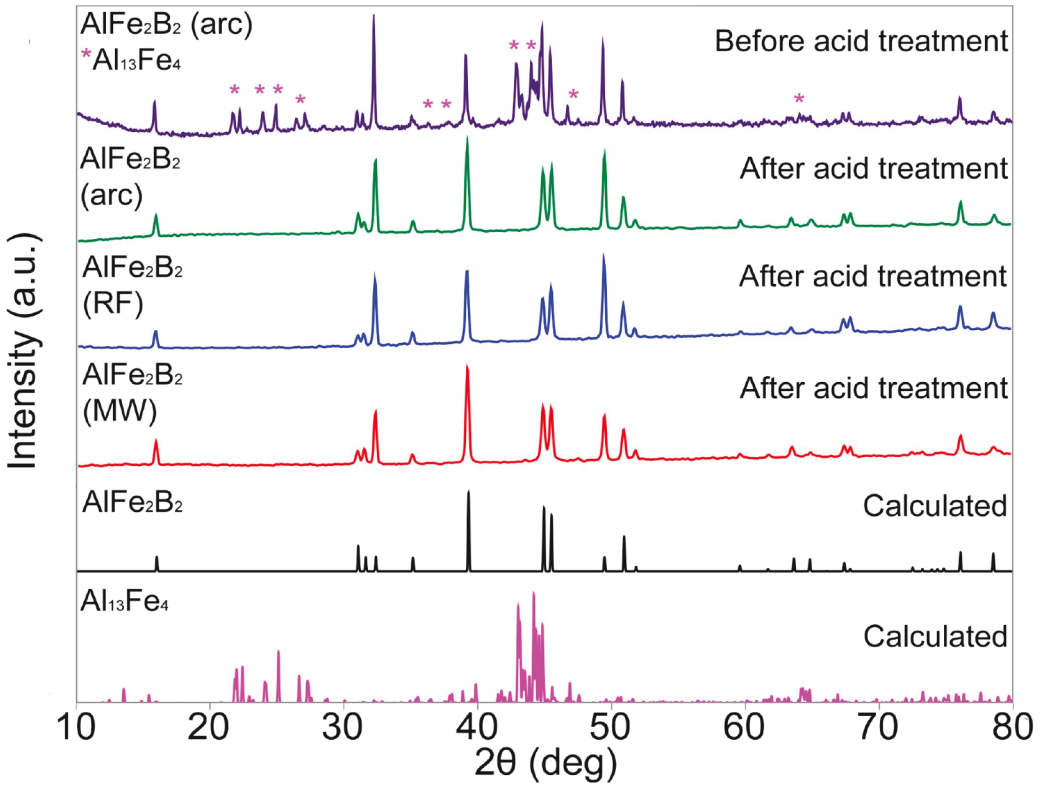


**Figure 1.** PXRD patterns of $AlFe_2B_2$ obtained by arc-, RF-, and MW-melting, followed by homogenizing annealing. The $Al_{13}Fe_4$ impurity peaks are labeled with asterisks. The calculated PXRD patterns for $AlFe_2B_2$ and $Al_{13}Fe_4$ are provided for comparison. The intensity redistribution, as compared to the calculated pattern of $AlFe_2B_2$, is caused by the texturing effect due to preferred faceting of crystallites parallel to the (0*k*0) planes.

reaction workup clearly demonstrates a dramatic improvement in the sample purity after treatment with HCl (Figure 1).

An alternative route to the synthesis of $AlFe_2B_2$ is RF-melting, which was used by Jeitschko in one of the first reported syntheses of this compound in 1969[17] (the other report, published in the same year, used the arc-melting technique[20]). We found that RF-melting also led to the presence of an $Al_{13}Fe_4$ impurity (Figure S1), which had to be removed by dissolution in dilute HCl. Once the ingot obtained by RF-melting a pelletized mixture of elements had been crushed and treated with HCl, the PXRD pattern of the resulting sample revealed a phase-pure $AlFe_2B_2$ (Figure 1).

The presence of the $Al_{13}Fe_4$ impurity is intrinsic to any synthetic protocol that aims to produce $AlFe_2B_2$ from Al-rich mixtures. The majority of works that reported phase-pure $AlFe_2B_2$ achieved their target by employing the postsynthetic treatment with dilute acid (Table 1). Strangely, another aspect of this synthesis appears to have been overlooked. Since $Al_{13}Fe_4$ forms as a byproduct, the reaction that uses an equimolar Fe/B ratio is inevitably nonstoichiometric with respect to the synthesis of $AlFe_2B_2$:

$$a\mathrm{Al} + b\mathrm{Fe} + c\mathrm{B} = p\mathrm{Al_{13}Fe_4} + q\mathrm{AlFe_2B_2} \quad (1)$$

It is easy to see that eq 1 simply cannot be balanced, because for any positive values of $p$ and $q$ we find that $b > c$; thus, the equimolar condition cannot be satisfied. Indeed, by performing PXRD analysis immediately after melting the mixtures of elements taken in the Al/Fe/B ratios of 3:2:2 (arc-melting[7]) or 7:7:6 (RF-melting[17]), we found traces of $AlB_2$ in the reaction products (Figure S2). Of course, the formation of $AlB_2$ can be attributed to the highly nonequilibrium conditions of these high-temperature synthetic procedures, but it can also be understood as the need to balance the formation of $Al_{13}Fe_4$, which decreases the Fe/B ratio below the value of 1, required for the stoichiometric formation of $AlFe_2B_2$. The homogenizing annealing at 900 °C led to the disappearance of the $AlB_2$ byproduct (at the level of PXRD sensitivity), which is likely explained by its reaction with some amount of $Al_{13}Fe_4$ to form more of $AlFe_2B_2$. Nevertheless, balancing eq 1 requires some other byproduct to be present in the reaction mixtures that used the equimolar or nearly equimolar Fe/B ratio in the nominal composition. We suggest that the annealed samples might contain traces of amorphous boron not detectable by the PXRD analysis.

With these considerations in mind, we decided to move away from the typical stoichiometry reported for the synthesis of $AlFe_2B_2$ by arc-melting or RF-melting and to follow the stoichiometry dictated by a balanced chemical equation, for example:

$$3\mathrm{Al} + 2.6\mathrm{Fe} + 2\mathrm{B} \approx 0.15\mathrm{Al_{13}Fe_4} + \mathrm{AlFe_2B_2} \quad (2)$$

We found that using such a stoichiometry results in the disappearance of the $AlB_2$ byproduct from the PXRD patterns recorded for the arc- or RF-melted samples prior to homogenizing annealing. Consequently, we used this stoichiometry to develop a new method for the synthesis of $AlFe_2B_2$.

An appealing alternative to the arc- and RF-melting methods is microwave (MW) synthesis,[18,25−28] which has been proven effective for the preparation of intermetallics compounds, e.g., $Ti_3SiC_2$,[29] $MnFe_2Si$,[30] and $Mg_2Sn$.[31] The MW heating provides for concentrated delivery of thermal energy to the metallic mixture.[32] Such rapid heating, however, should be carefully controlled to avoid an implosion of the evacuated tube that


https://dx.doi.org/10.1021/acs.inorgchem.0c01731
Inorg. Chem. 2020, 59, 12625−12631

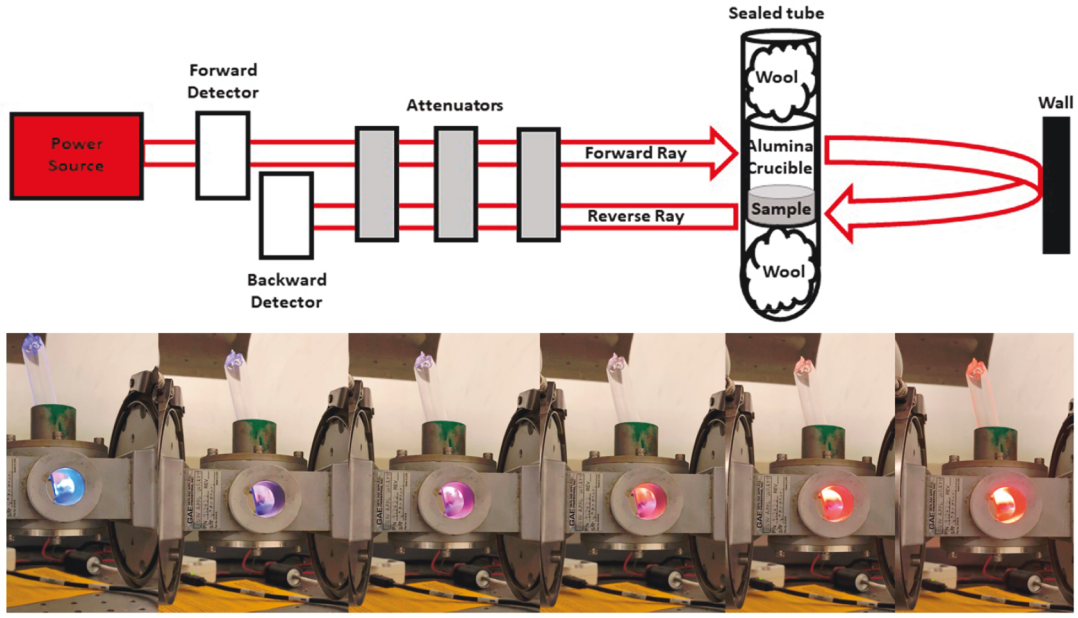


**Figure 2.** Scheme of the microwave reactor setup and the visual progression of the synthesis of $AlFe_2B_2$ in the MW cavity as a function of time from left to right.

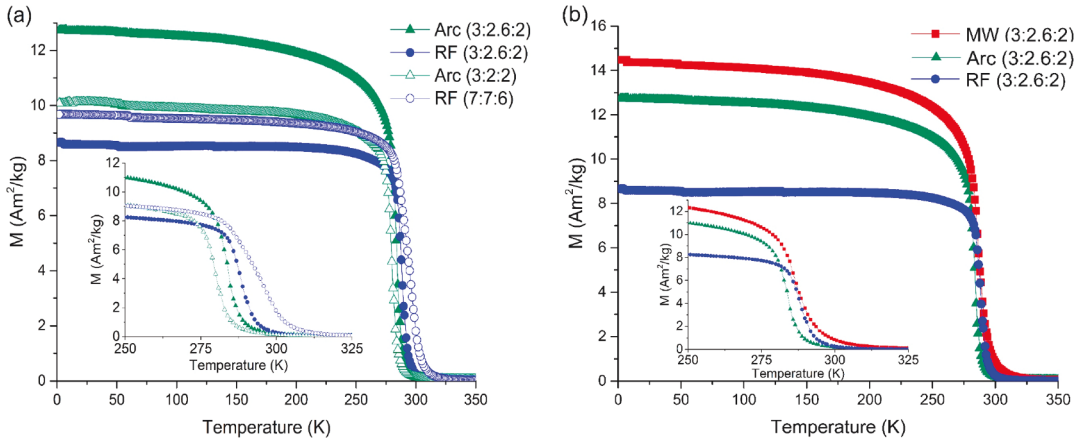


**Figure 3.** Temperature dependence of field-cooled magnetization of $AlFe_2B_2$ for the arc- and RF-melted samples prepared with different Al/Fe/B ratios (a) and for the arc-, RF-, and MW-melted samples prepared with the same ratio (b). The insets show an enlarged portion of the plots near the FM ordering temperature.

encloses the crucible with the reactants. We found that adding glass wool above and below the alumina crucible provides sufficient heat insulation, making the quartz tube stable for a longer time. The mixture of elements taken in the Al/Fe/B ratio of 3:2.6:2 was subjected to 5 min of heating in a 0.5 kW MW reactor, which led to the fast increase in the temperature of the reactants (Figure 2). After homogenizing annealing at 900 °C, PXRD revealed $AlFe_2B_2$ as the major phase and $Al_{13}Fe_4$ as a byproduct (Figure S1), which was eliminated by treatment with dilute HCl to yield a phase-pure $AlFe_2B_2$ (Figure 1).

When the three methodologies discussed in this paper are compared, all of them are valid methods for the synthesis of $AlFe_2B_2$, although an additional treatment with acid is required to achieve a phase-pure sample. Given the interest of $AlFe_2B_2$ as a promising magnetic refrigerant, we decided to compare the magnetic and magnetocaloric properties of the materials obtained by different synthetic techniques.

**Magnetic Properties and Magnetocaloric Effect.** Magnetic measurements performed on the samples that were synthesized using the earlier reported Al/Fe/B ratios of 3:2:2 (arc-melting) and 7:7:6 (RF-melting) revealed the FM ordering at $T_C$ = 280 and 293 K, respectively (Figure 3a; the $T_C$ values were determined from the Arrott plots shown in Figure S3). On the other hand, the arc-melted and RF-melted samples prepared with the 3:2.6:2 ratio showed $T_C$ = 286 and 287 K, respectively, which was similar to $T_C$ = 287 K determined for the MW-melted sample prepared with the same ratio (Figure 3b). Recently, Lejeune et al. have shown that the $T_C$ for $AlFe_2B_2$ is sensitive to antisite defects that result in a narrow stoichiometry range according to the formula $Al_{1-y}Fe_{2+y}B_2$ ($-0.01 \leq y \leq 0.01$).[33] Despite the narrowness of this range, it has been established that the $T_C$ value increases from 280 to 315 K as the Al/Fe ratio decreases. These findings explain the variation in $T_C$ observed for our samples: the decrease in the Al/Fe loading ratio also leads to higher FM


https://dx.doi.org/10.1021/acs.inorgchem.0c01731
Inorg. Chem. 2020, 59, 12625−12631

ordering temperatures, while the samples prepared with the same loading ratio of 3:2.6:2 show very similar $T_C$ values (Table 2). Thus, although the excess of Al is used in these reactions to suppress the formation of the FeB byproduct, while the $Al_{13}Fe_4$ byproduct is subsequently removed by acid treatment, it appears, quite reasonably, that the larger excess of Al favors Al-enriched antisite defects ($y < 0$) in $Al_{1-y}Fe_{2+y}B_2$.

**Table 2. Magnetic Properties of the Samples of $AlFe_2B_2$ Prepared by Different Methods**

| synthetic method | Al/Fe/B ratio | $T_c$, K | $-\Delta S_M$, J kg$^{-1}$ K$^{-1}$ (2 T/5 T) |
|---|---|---|---|
| arc-melting | 3:2:2 | 280 | ~2.62/5.56 |
| | 3:2.6:2 | 286 | 3.75/7.21 |
| RF-melting | 7:7:6 | 293 | ~3.10/6.75 |
| | 3:2.6:2 | 287 | 3.38/6.47 |
| MW-melting | 3:2.6:2 | 287 | 3.31/6.45 |

The influence of the Al/Fe loading ratio on the magnetic properties can also be seen in the evolution of field-dependent magnetization measured at 1.8 K. The saturation magnetization values found for the arc-melted sample with the Al/Fe/B = 3:2:2 ratio and the RF-melted one with the 7:7:6 ratio were 0.93 and 1.28 $\mu_B$ per Fe atom, respectively (Figure 4a). In contrast, the values found for the arc-, RF-, and MW-melted samples prepared with the 3:2.6:2 ratio were more consistent, 1.23, 1.13, and 1.11 $\mu_B$ per Fe atom, respectively (Figure 4b). These values are comparable to the range of magnetization values reported for $AlFe_2B_2$.[12]

The magnetocaloric effect was measured as a magnetic entropy change ($\Delta S_m$) calculated for each sample from a set of magnetization isotherms (Figure S3) collected within the range of 40 K below and above the $T_C$ value. The Maxwell eq 3 was approximated with the sum (4):

$$\Delta S_m(T, \Delta H) = \int_0^{H_{max}} \left(\frac{\partial M}{\partial T}\right)_H dH \quad (3)$$

$$\Delta S_m(T_i, \Delta H) = \sum_0^{H_{max}} \frac{M_i - M_{i-1}}{T_i - T_{i-1}} \Delta H \quad (4)$$

where $T_i - T_{i-1}$ is the incremental change in temperature, $M_i - M_{i-1}$ is the incremental change in magnetization, and $\Delta H$ is the change in the magnetic field. Using eq 4, $-\Delta S_m$ was calculated for each sample for $H_{max}$ = 2 and 5 T (Table 2).

The change in the Al/Fe loading ratio, clearly, results in the large variation in the $T_C$ and $-\Delta S_m$ values, with the Al-richer content being detrimental to the MCE (Figure 5a). Even taking into account the substantial error involved in the indirect MCE measurement with eq 4, the decrease in the magnitude of the MCE peak for the arc-melted sample with the Al/Fe/B ratio of 3:2:2 is obvious. Keeping the same loading ratio, Al/Fe/B = 3:2.6:2, results in more consistent MCE values as shown by the comparison of samples prepared by different methods (Figure 5b). Among these, the maximum MCE was observed for the arc-melted sample, $-\Delta S_m$ = 3.75 J·kg$^{-1}$·K$^{-1}$ at $H_{max}$ = 2 T and $-\Delta S_m$ = 7.21 J·kg$^{-1}$·K$^{-1}$ at $H_{max}$ = 5 T, with the values for the RF- and MW-melted samples being only slightly lower. These values are in good agreement with those previously reported by us[7] and other groups.[15,33−35]

## CONCLUSIONS

This work demonstrates the utility of three different synthetic routes for the preparation of $AlFe_2B_2$, with the introduction of microwave (MW) melting as a new technique for the synthesis of this material. The magnetic and magnetocaloric properties of the MW-melted sample are similar to those measured on the arc- and RF-melted samples, as long as the samples are prepared with the same Al/Fe/B loading ratio. The increase in the Al loading results in the decrease in the ferromagnetic ordering temperature ($T_C$) and deterioration of magnetocaloric properties. Such behavior is well explained by the recently demonstrated influence of minor deviations from the ideal 1:2:2 stoichiometry on the $T_C$ value of $AlFe_2B_2$. Interestingly, the change in the synthetic method has a relatively weak influence on the magnetic ordering and magnetocaloric effect.

We also find that, from the synthetic point of view, the initial loading that uses an equimolar Fe/B ratio is not optimal for the synthesis of $AlFe_2B_2$. Indeed, the intentional formation of the $Al_{13}Fe_4$ byproduct, to avoid the presence of a ferromagnetic FeB impurity, necessitates the use of nominal loadings with Fe/B > 1 to satisfy the reaction stoichiometry. It will be interesting to explore this oversight in the synthesis of $AlFe_2B_2$ to understand whether the stoichiometrically correct synthesis can be used to improve the yield of the target phase and how it

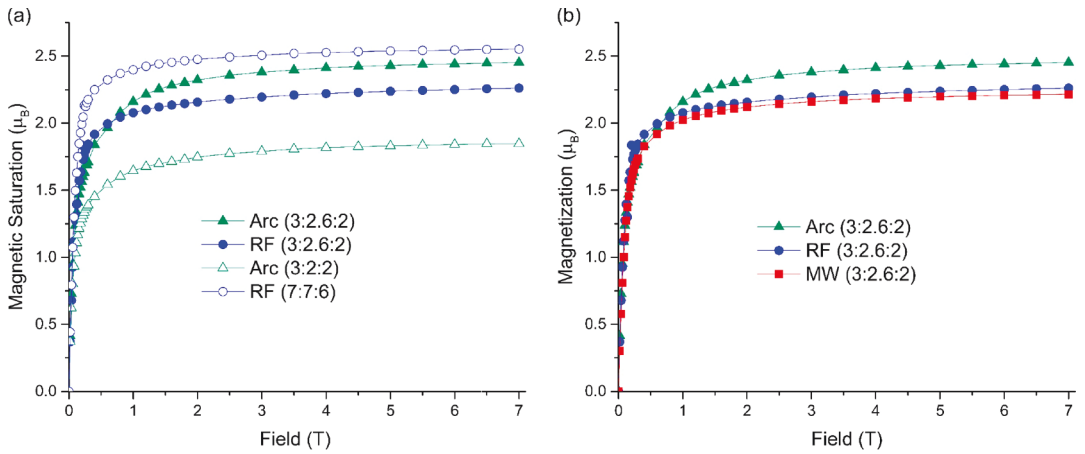


**Figure 4.** Field-dependent magnetization of $AlFe_2B_2$ measured at 1.8 K for the arc- and RF-melted samples prepared with different Al/Fe/B ratios (a) and for the arc-, RF-, and MW-melted samples prepared with the same ratio (b).


https://dx.doi.org/10.1021/acs.inorgchem.0c01731
Inorg. Chem. 2020, 59, 12625−12631

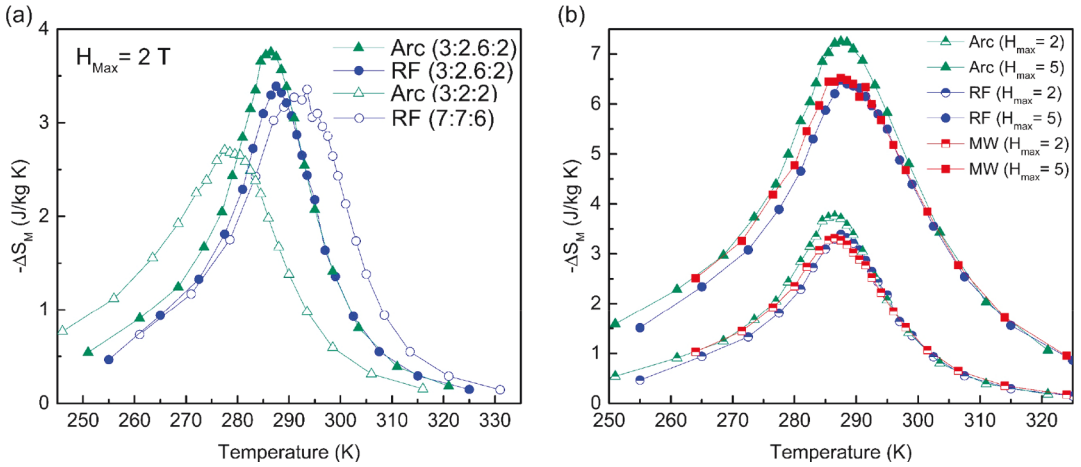


**Figure 5.** Magnetic entropy change of $AlFe_2B_2$ calculated for the indicated magnetic field change for the arc- and RF-melted samples prepared with different Al/Fe/B ratios (a) and for the arc-, RF-, and MW-melted samples prepared with the same ratio of 3:2.6:2 (b).

can influence the magnetic properties. Results of such studies will be reported in due course.

## ■ ASSOCIATED CONTENT

### Supporting Information

The Supporting Information is available free of charge at https://pubs.acs.org/doi/10.1021/acs.inorgchem.0c01731.

Additional PXRD patterns; the isotherms used to calculate the magnetocaloric effect; SEM images (PDF)

## ■ AUTHOR INFORMATION


### Corresponding Author

**Michael Shatruk** − *Department of Chemistry and Biochemistry, Florida State University, Tallahassee, Florida 32306, United States; National High Magnetic Field Laboratory, Tallahassee, Florida 32310, United States;* orcid.org/0000-0002-2883-4694; Email: mshatruk@fsu.edu

### Authors

**Dallas K. Mann** − *Department of Chemistry and Biochemistry, Florida State University, Tallahassee, Florida 32306, United States*

**YiXu Wang** − *Department of Chemistry and Biochemistry, Florida State University, Tallahassee, Florida 32306, United States; School of Materials Science and Engineering, University of Science and Technology Beijing, Beijing 100083, P.R. China*

**Jeanette D. Marks** − *Department of Chemistry and Biochemistry, Florida State University, Tallahassee, Florida 32306, United States; Sarasota Military Academy, Sarasota, Florida 34236, United States*

**Geoffrey F. Strouse** − *Department of Chemistry and Biochemistry, Florida State University, Tallahassee, Florida 32306, United States;* orcid.org/0000-0003-0841-282X

Complete contact information is available at: https://pubs.acs.org/10.1021/acs.inorgchem.0c01731


### Notes

The authors declare no competing financial interest.

## ■ ACKNOWLEDGMENTS

This research was supported by the National Science Foundation (award DMR-1905499 to M.S.) and in part by the Air Force Office of Scientific Research (award CRADA-039811 to G.F.S.). Y.X.W. acknowledges the Chinese Scholarship Council for supporting his visit to Florida State University (award No. 201706460046). J.D.M. was supported by the Research Experience for Teachers program administered by the National High Magnetic Field Laboratory, which is supported by the National Science Foundation Cooperative Agreement No. DMR-1644779 and the state of Florida.

## ■ REFERENCES


(1) Moya, X.; Kar-Narayan, S.; Mathur, N. D. Caloric materials near ferroic phase transitions. *Nat. Mater.* **2014**, *13*, 439−450.

(2) Weiss, P.; Piccard, A. Le phénomène magnétocalorique. *J. Phys. Theor. Appl.* **1917**, *7*, 103−109.

(3) Pecharsky, V. K.; Gschneidner, K. A., Jr. Giant magnetocaloric effect in $Gd_5(Si_2Ge_2)$. *Phys. Rev. Lett.* **1997**, *78*, 4494−4497.

(4) Franco, V.; Blázquez, J. S.; Ingale, B.; Conde, A. The magnetocaloric effect and magnetic refrigeration near room temperature: materials and models. *Annu. Rev. Mater. Res.* **2012**, *42*, 305−342.

(5) Biswas, A.; Pathak, A. K.; Zarkevich, N. A.; Liu, X.; Mudryk, Y.; Balema, V.; Johnson, D. D.; Pecharsky, V. K. Designed materials with the giant magnetocaloric effect near room temperature. *Acta Mater.* **2019**, *180*, 341−348.

(6) Morrison, K.; Lyubina, J.; Moore, J. D.; Sandeman, K. G.; Gutfleisch, O.; Cohen, L. F.; Caplin, A. D. Magnetic refrigeration: phase transitions, itinerant magnetism and spin fluctuations. *Philos. Mag.* **2012**, *92*, 292−303.

(7) Tan, X.; Chai, P.; Thompson, C. M.; Shatruk, M. Magnetocaloric effect in $AlFe_2B_2$: toward magnetic refrigerants from earth-abundant elements. *J. Am. Chem. Soc.* **2013**, *135*, 9553−9557.

(8) Chai, P.; Stoian, S. A.; Tan, X. Y.; Dube, P. A.; Shatruk, M. Investigation of magnetic properties and electronic structure of layered-structure borides $AlT_2B_2$ (T = Fe, Mn, Cr) and $AlFe_{2-x}Mn_xB_2$. *J. Solid State Chem.* **2015**, *224*, 52−61.

(9) Cedervall, J.; Andersson, M. S.; Sarkar, T.; Delczeg-Czirjak, E. K.; Bergqvist, L.; Hansen, T. C.; Beran, P.; Nordblad, P.; Sahlberg, M. Magnetic structure of the magnetocaloric compound $AlFe_2B_2$. *J. Alloys Compd.* **2016**, *664*, 784−791.

(10) (a) Lewis, L. H.; Barua, R.; Lejeune, B. Developing magnetofunctionality: Coupled structural and magnetic phase transition in $AlFe_2B_2$. *J. Alloys Compd.* **2015**, *650*, 482−488. (b) Oey, Y. M.; Bocarsly, J. D.; Levin, E. E.; Mann, D.; Shatruk, M.; Seshadri, R. Structural changes upon magnetic ordering in magnetocaloric $AlFe_2B_2$. *Appl. Phys. Lett.* **2020**, *116*, 212403.

(11) Levin, E. M.; Jensen, B. A.; Barua, R.; Lejeune, B.; Howard, A.; McCallum, R. W.; Kramer, M. J.; Lewis, L. H. Effects of Al content

and annealing on the phases formation, lattice parameters, and magnetization of $Al_xFe_2B_2$ (x = 1.0,1.1,1.2) alloys. *Phys. Rev. Mater.* **2018**, *2*, No. 034403.
(12) Kota, S.; Sokol, M.; Barsoum, M. W. A progress report on the MAB phases: atomically laminated, ternary transition metal borides. *Int. Mater. Rev.* **2020**, *65*, 226−255.
(13) Lamichhane, T. N.; Xiang, L.; Lin, Q.; Pandey, T.; Parker, D. S.; Kim, T.-H.; Zhou, L.; Kramer, M. J.; Bud'ko, S. L.; Canfield, P. C. Magnetic properties of single crystalline itinerant ferromagnet $AlFe_2B_2$. *Phys. Rev. Mater.* **2018**, *2*, No. 084408.
(14) Ade, M.; Hillebrecht, H. Ternary borides $Cr_2AlB_2$, $Cr_3AlB_4$, and $Cr_4AlB_6$: the first members of the series $(CrB_2)_nCrAl$ with $n$ = 1, 2, 3 and a unifying concept for ternary borides as MAB-phases. *Inorg. Chem.* **2015**, *54*, 6122−6135.
(15) Hirt, S.; Yuan, F.; Mozharivskyj, Y.; Hillebrecht, H. $AlFe_{2-x}Co_xB_2$ ($x$ = 0−0.30): $T_C$ tuning through Co substitution for a promising magnetocaloric material realized by spark plasma sintering. *Inorg. Chem.* **2016**, *55*, 9677−9684.
(16) Du, Q.; Chen, G.; Yang, W.; Wei, J.; Hua, M.; Du, H.; Wang, C.; Liu, S.; Han, J.; Zhang, Y.; Yang, J. Magnetic frustration and magnetocaloric effect in $AlFe_{2-x}Mn_xB_2$ ($x$ = 0−0.5) ribbons. *J. Phys. D: Appl. Phys.* **2015**, *48*, 335001.
(17) Jeitschko, W. Crystal structure of $Fe_2AlB_2$. *Acta Crystallogr., Sect. B: Struct. Crystallogr. Cryst. Chem.* **1969**, *25*, 163−165.
(18) Kitchen, H. J.; Vallance, S. R.; Kennedy, J. L.; Tapia-Ruiz, N.; Carassiti, L.; Harrison, A.; Whittaker, A. G.; Drysdale, T. D.; Kingman, S. W.; Gregory, D. H. Modern microwave methods in solid-state inorganic materials chemistry: from fundamentals to manufacturing. *Chem. Rev.* **2014**, *114*, 1170−1206.
(19) *X'Pert HighScore Plus software*, v. 2.2b; PANalytical B.V.: Almelo, Netherlands, 2006.
(20) Kuz'ma, Y.; Chaban, N. F. Crystalline structure of $Fe_2AlB_2$. *Izv. Akad. Nauk SSSR, Neorg. Mater.* **1969**, *5*, 384−385.
(21) Mann, D. K.; Xu, J.; Mordvinova, N. E.; Yannello, V.; Ziouani, Y.; González-Ballesteros, N.; Sousa, J. P. S.; Lebedev, O. I.; Kolen'ko, Y. V.; Shatruk, M. Electrocatalytic water oxidation over $AlFe_2B_2$. *Chem. Sci.* **2019**, *10*, 2796−2804.
(22) Ali, T.; Khan, M. N.; Ahmed, E.; Ali, A. Phase analysis of $AlFe_2B_2$ by synchrotron X-ray diffraction, magnetic and Mössbauer studies. *Prog. Nat. Sci.* **2017**, *27*, 251−256.
(23) Cedervall, J.; Häggström, L.; Ericsson, T.; Sahlberg, M. Mössbauer study of the magnetocaloric compound $AlFe_2B_2$. *Hyperfine Interact.* **2016**, *237*, 47.
(24) Kádas, K.; Iuşan, D.; Hellsvik, J.; Cedervall, J.; Berastegui, P.; Sahlberg, M.; Jansson, U.; Eriksson, O. $AlM_2B_2$(M = Cr, Mn, Fe, Co, Ni): a group of nanolaminated materials. *J. Phys.: Condens. Matter* **2017**, *29*, 155402.
(25) Gerbec, J. A.; Magana, D.; Washington, A.; Strouse, G. F. Microwave-Enhanced Reaction Rates for Nanoparticle Synthesis. *J. Am. Chem. Soc.* **2005**, *127*, 15791−15800.
(26) Washington, A. L., II; Strouse, G. F. Microwave synthesis of CdSe and CdTe nanocrystals in nonabsorbing alkanes. *J. Am. Chem. Soc.* **2008**, *130*, 8916−8922.
(27) Washington, A. L.; Strouse, G. F. Microwave Synthetic Route for Highly Emissive TOP/TOP-S Passivated CdS Quantum Dots. *Chem. Mater.* **2009**, *21*, 3586−3592.
(28) Levin, E. E.; Grebenkemper, J. H.; Pollock, T. M.; Seshadri, R. Protocols for high temperature assisted-microwave preparation of inorganic compounds. *Chem. Mater.* **2019**, *31*, 7151−7159.
(29) Dmitruk, A.; Naplocha, K.; Lagos, M.; Egizabal, P.; Grzeda, J. Microwave assisted self-propagating high-temperature synthesis of $Ti_3SiC_2$ max phase. *Compos. Theory Pract.* **2018**, *18*, 241−244.
(30) Bocarsly, J. D.; Levin, E. E.; Garcia, C. A. C.; Schwennicke, K.; Wilson, S. D.; Seshadri, R. A simple computational proxy for screening magnetocaloric compounds. *Chem. Mater.* **2017**, *29*, 1613−1622.
(31) Fan, Z.; Cappelluti, M. D.; Gregory, D. H. Ultrafast, energy-efficient synthesis of intermetallics; microwave-induced metal plasma (MIMP) synthesis of $Mg_2Sn$. *ACS Sustainable Chem. Eng.* **2019**, *7*, 19686−19698.
(32) Siebert, J. P.; Hamm, C. M.; Birkel, C. S. Microwave heating and spark plasma sintering as non-conventional synthesis methods to access thermoelectric and magnetic materials. *Appl. Phys. Rev.* **2019**, *6*, No. 041314.
(33) Lejeune, B. T.; Schlagel, D. L.; Jensen, B. A.; Lograsso, T. A.; Kramer, M. J.; Lewis, L. H. Effects of Al and Fe solubility on the magnetofunctional properties of $AlFe_2B_2$. *Phys. Rev. Mater.* **2019**, *3*, No. 094411.
(34) Barua, R.; Lejeune, B. T.; Jensen, B. A.; Ke, L.; McCallum, R. W.; Kramer, M. J.; Lewis, L. H. Enhanced room-temperature magnetocaloric effect and tunable magnetic response in Ga-and Ge-substituted $AlFe_2B_2$. *J. Alloys Compd.* **2019**, *777*, 1030−1038.
(35) Zhang, Z.; Yao, G.; Zhang, L.; Jia, P.; Fu, X.; Cui, W.; Wang, Q. Magnetic phase transition and room-temperature magnetocaloric effects in $(Al,M)Fe_2B_2$ (M = Si, Ga) compounds. *J. Magn. Magn. Mater.* **2019**, *484*, 154−158.


https://dx.doi.org/10.1021/acs.inorgchem.0c01731
*Inorg. Chem.* 2020, 59, 12625−12631